Eur. Phys. J. A **4**, 147–155 (1999)

THE EUROPEAN PHYSICAL JOURNAL A

De–excitation of compound nuclei with A around 56: reduction of the emission barriers for protons and alpha particles

P. Jänker[a], H. Leitz[b], K.E.G. Löbner[c], M. Moralles[d], H.G. Thies[b]

Sektion Physik, University of Munich, D-85748 Garching, Germany

Received: 15 June 1998 / Revised version: 5 November 1998
Communicated by C. Signorini

Abstract. This paper contributes to the discussion on the phenomena of the enhanced emission of low–energetic charged particles during compound nuclei decay. The decay of compound nuclei ^{52}Fe, ^{56}Ni, and ^{59}Cu was studied. Energy spectra and emission angles of evaporated charged particles were measured in coincidence with gamma rays to determine the corresponding evaporation residue nucleus. Additionally, evaporation residue distributions were determined with the Munich rf recoil spectrometer. In this way, detailed channel–specific evaporation data were obtained for theoretical analysis. We extracted evaporation barriers and compared them with corresponding fusion barriers. The main result was revealed to be a lowering of the evaporation barrier for protons and alpha particles relative to the fusion barriers. But the observed effect is not as intensive as reported in recent studies.

PACS. 24.10.-i Nuclear–reaction models and methods – 25.60.Pj Fusion reactions – 25.70.Gh Compound nucleus

1 Introduction

A topic in current heavy ion research undergoing lively discussion is the phenomena of reduced emission barriers for light charged particles during the decay of compound nuclei. Experimental evidence for this phenomena is reported in various papers [e.g. 1 and references therein]. The study by Parker et al. [1] deals with the decay of compound nuclei over a wide range of nuclear charges from Z = 16 to 64. The paper presented experimental energy spectra of evaporated particles showing an excess of low–energetic particles in comparison with results of statistical model calculations. These differences were interpreted by the authors as being due to reduced emission barriers for protons and alpha particles. As an example, experimental data concerning the reaction 167 MeV ^{20}Ne +^{12}C were interpreted as being due to proton barriers lowered by 80 %. Extreme deformations of the emitter nuclei were suspected. However, there is controversy about the magnitude of this effect. Some authors [2,3] were able to reproduce experimental data [4,5], respectively, by assuming that the emitter nuclei are spherical in shape, and questioned the correct interpretation of the data. Further, Gollerthan et al. [6], who carried out a detailed channel–specific study on the decay of the compound nucleus ^{179}Au, established that the emission barriers were reduced only moderately.

There are some shortcomings with regard to the experiments published, which reveal a drastic reduction of emission barriers: most of them were based on inclusive measurements, without determination of the decay channel. Thus, background due to reactions with "impurities" like H, O, C could have falsified the energy spectra. We infer, that channel–specific experiments are necessary to overcome this problem.

2 Experiments

In order to obtain a comprehensive amount of experimental information, we carried out two series of experiments:

- channel-specific energy and angular distributions of evaporated, light charged particles (γ particle coincidence experiments);
- determination of evaporation residue distributions (rf recoil spectrometer measurements [7]).

[a] present address: Daimler Chrysler, Research and Technology, D-81663 München, Germany
[b] present address: Skyways Flugreisen GmbH, Germaniastr. 11, D–80802 München, Germany
[c] Corresponding author e–mail: loebner@physik.uni–muenchen.de
[d] present address Divisao de Fisica Nuclear IPEN/CNEN–SP, Caixa Postal 11049, CEP 05422–970 – Sao Paulo – SP, Brazil

We chose the reactions: ^{40}Ca + ^{12}C, ^{16}O, ^{19}F with typical excitation energies of 1 MeV/u (39, 55, and 59 MeV, respectively).

2.1 γ particle coincidence experiments – experimental setup

A 350 μg/cm^2 ^{40}Ca target was bombarded with pulsed ^{12}C (33.8 MeV), ^{16}O (64.0 MeV)and ^{19}F (53.5 MeV) beams from the Munich tandem accelerator. The energy spectra and angular distributions of light charged particles were measured in coincidence with γ–rays. These kinematics are advantageous because of low center–of–mass velocities.

A multi-detector system was developed specially for these experiments. It is sketched in Fig. 1. This detector system consists of a Ge γ–ray detector and 21 particle ΔE-E$_{res}$ telescopes. The particle telescopes are arranged on a sphere around the target position. They were installed at backward angles, causing negligible kinematical errors, and thresholds for energy measurement were low. Figure 1 shows the telescope design. We used PIN diodes, large–area (100 mm^2) photo detectors. The front detector, 200 μm thick, has an aluminum-coated (1.2 μm) entrance and gold-coated (0.35 μm) rear side. A fast timing signal was attained with a 50–Ohm microwave-amplifier circuit connected to the cathode. A conventional charge-sensitive pre–amplifier was connected to the anode for energy read–out.

In order to achieve a sufficiently thick E$_{res}$ detector for stopping higher–energetic particles, three 380-μm-thick PIN diodes were stacked together. It was proved that energy resolution of this configuration does not suffer due to the threefold electrical capacity of the detector.

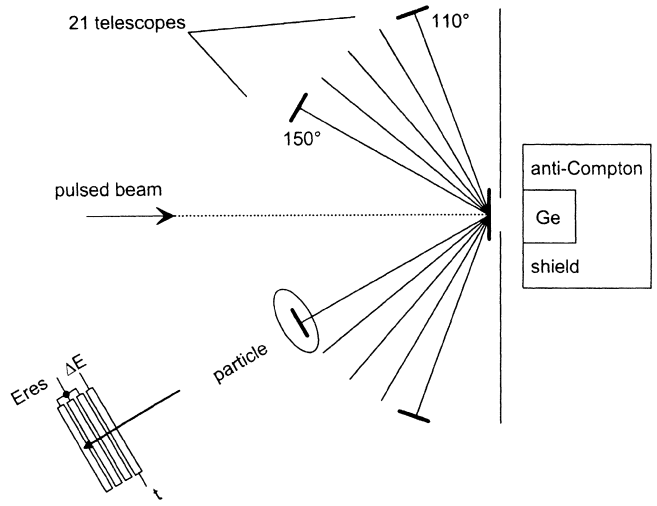

Fig. 1. Multi–detector system. 21 particle telescopes for applying ΔE-E$_{res}$ as well as time–of–flight techniques are arranged at backward angles on a sphere around the target. An anti–Compton–shielded γ–ray Ge detector was installed for single and coincidence measurements

The telescopes were tested with low–energy proton and alpha particle beams from the Van–de–Graaff accelerator at the Max Planck Institute for Plasmaphysics and the Munich tandem accelerator (energies from 0.5 MeV up to 13 MeV). Based on these measurements, an energy–calibration method was worked out regarding passive zones of the diodes. Figure 2 indicates good energy–resolution performance of the telescopes. The energy resolution was better than 30 keV for 6.8 MeV alpha–particles.

Two methods of particle identification were advantageously combined : ΔE-E$_{res}$ and time–of–flight measurement. Low–energetic particles, stopped in the ΔE detectors, were identified through time–of–flight measurements relative to the pulsed beam. Higher–energetic particles were identified by the ΔE-E$_{res}$ method. Consequently, technical disadvantages inherent in the individual methods were avoided: the ΔE-E$_{res}$ method requires extremely thin ΔE detectors to resolve low–energetic particles, and extremely good time resolution is needed for the time–of–flight identification of high-energetic particles.

Excellent timing resolution was achieved with the detector system: 160 ps fwhm with a pulsed beam using the post-acceleration buncher at the Munich Tandem Laboratory. This allowed positioning the detectors close to the target – 45 mm away – achieving a large total solid angle of 0.5 sr.

To obtain channel–specific light charged particle energy and angular distributions, γ–rays were measured in coincidence. We used an anti-Compton shielded γ–spectrometer. This spectrometer consists of a large germanium crystal with a relative efficiency of 30% surrounded by veto–detector BGO crystals enclosing the germanium crystal in the form of a cylinder, and an additional NaI(Tl) disk.

Considerable effort was expended on the design and manufacture of the target. We used a composite target to avoid Doppler broadening. 350 μg/cm^2 ^{40}Ca was vapor–deposited on a ^{120}Sn foil. This foil was thick enough to stop reaction products and thin enough to let projectile particles pass. A 50 μg/cm^2 gold layer was evaporated on the Ca side of the target in order to avoid oxidation. The projectile particles passing the target are stopped in a Pb foil arranged closely in front of the γ–ray detector. The special target and the optimized geometry of the experimental setup reduced the rate of scattered projectile particles in the particle telescopes effectively. A coincidence logic circuit was designed to record only γ–particle–coincident events. The telescopes and the corresponding electronics were calibrated with an electronic charge injector and with an alpha source before and after all experiments.

2.2 Rf recoil spectrometer measurements – experimental setup

The Munich rf recoil spectrometer [7] was used to measure the evaporation residue distributions. Self–supporting 72 μg/cm^2 C and 100 μg/cm^2 SiO_2 targets and a 185 μg/cm^2 CaF_2 target vapor–deposited on a 150 μg/cm^2 Ni foil were

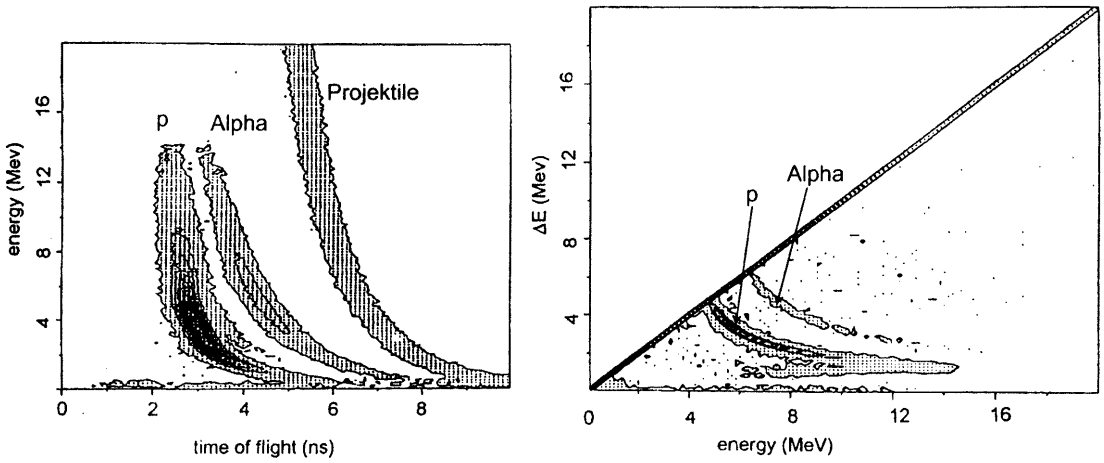

Fig. 2. Resolution of the telescopes: The right side shows ΔE-E$_{res}$ results, and the left side energy vs. time of flight

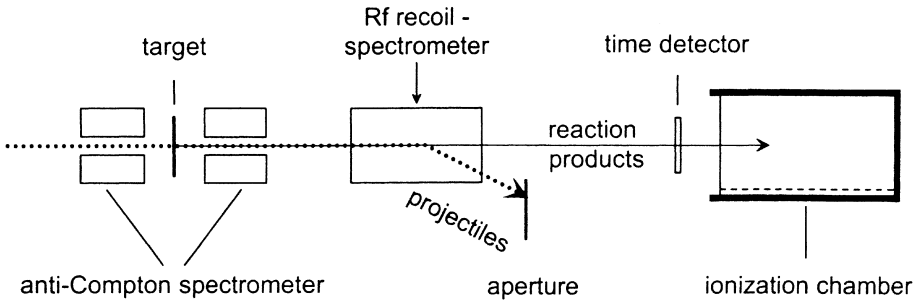

Fig. 3. The Munich rf recoil spectrometer. Combination of a magnetic deflection system and a 20 kW 15 MHz rf–operated deflector

bombarded with a pulsed ^{40}Ca beam from the Munich tandem accelerator. The bombarding energy of the projectile beam was 112.7 MeV for the reaction ^{40}Ca + ^{12}C, 110 and 137 MeV for ^{40}C + ^{16}O and 112.7 Mev for the reaction ^{40}C + ^{12}F.

The Munich rf recoil spectrometer permits separating and identifying reaction products at 0^o. The setup is sketched in Fig. 3. The main component of the spectrometer is a radio–frequency–operated velocity filter which separates the slower reaction products from the faster projectile particles. Reaction products are identified by a combination of a large-window ΔE-E$_{res}$ ionization chamber and a time–of–flight detector (channel plate) measuring the time of flight relative to the pulsed beam. These detectors are positioned at 0^o.

The selected inverse reaction kinematics with high kinetic energies of the evaporation residues yield two advantages: (1) high Z-resolution with the ionization chamber, and (2) good focus of the reaction products which means high acceptance of the recoil spectrometer.

The detection efficiency of the recoil spectrometer is channel–dependent. In particular, evaporation of alpha particles scatters the nuclei and reduces the detection efficiency. The detection efficiencies were determined in order to correct this effect in the analysis. For this purpose an independent detector system was installed: two γ–ray detectors, each equipped with an anti-Compton shield. This allows coincident and single measurements. A special target coated with Pb was used for single γ-measurements. The Pb layer served to stop evaporation of the residue nuclei before emitting γ–rays in order to avoid Doppler broadening.

3 Data analysis

3.1 γ particle coincidence data

The analysis of the recorded data included the following steps:

1. The evaporated particle or particles were identified by a computer routine applying the ΔE-E$_{res}$ or time-of-flight identification method.
2. The energy of the evaporated particle/particles was calculated by a routine taking into account all the passive layers of the telescopes concerned. Energy–loss calculations were performed applying semi–empirical formulas from the compilation by Anderson and Ziegler [8].
3. The particle energy was transformed from the lab into the center–of–mass system, assuming two–body kinematics. Monte–Carlo simulations were performed to prove that the errors involved in this method are negligible.
4. Particle energy spectra were accumulated for different γ–energy intervals. Raw channel–specific spectra were produced by choosing narrow analysis intervals around

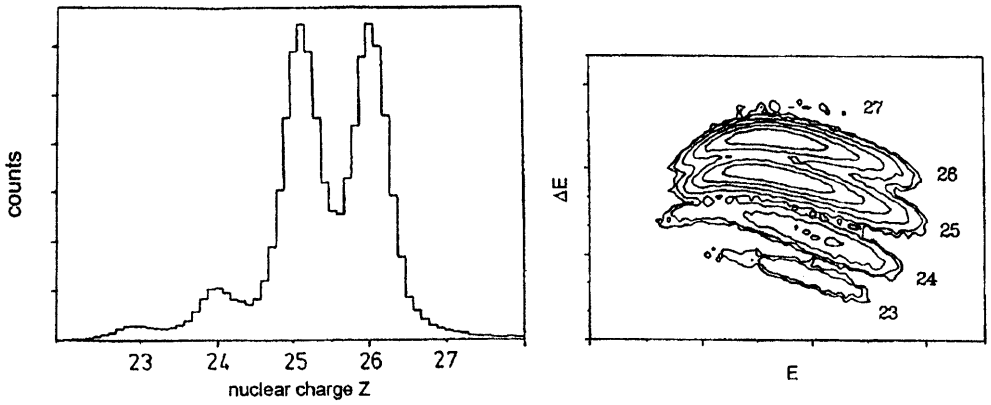

Fig. 4. Detection of evaporation residue nuclei with the Munich rf recoil spectrometer: The right side shows ΔE-E_{res} results, and the left side the corresponding Z-distribution for the 110 MeV ^{40}Ca + ^{16}O experiment

characteristic γ–peaks. Background spectra were generated by choosing energy regions between the characteristic peaks.

5. Pure channel–specific spectra were generated by subtracting background spectra from the raw channel–specific spectra. The consistency of this method was proved by comparing energy spectra belonging to different characteristic gamma rays of the same isotope.
6. The spectra were corrected by energy–dependent transformation of the solid angle of the detector from the lab to the center–of–mass system [9].
7. The results of the individual telescopes were compared for angle–dependent effects, and finally summed up.

A consistent experimental finding was attained by cross–checking spectra from different detectors accumulated under all the different analysis conditions.

3.2 Rf recoil spectrometer measurements

The nuclear charge of the evaporation residues was obtained from the ΔE and total energy E using a second–order function Z(ΔE, E_{res}) in ΔE and E_{res}. The nuclear mass A was calculated from the total kinetic energy and time of flight. The resolution of the instrument is shown in Fig. 4.

The γ data were analyzed by determining the relative intensities of nuclei–specific γ–peaks N_{gij} (i indicates the nucleus and j the γ–peak). Then, coincidence conditions were set to determine the rates Nc_{ij} of γ and recoil–spectrometer–coincident events. The channel–specific detection efficiencies of the rf recoil spectrometer $\epsilon_i = Nc_{ij}/N_{gij}$ were calculated by comparing N_{gij} and Nc_{gij}. The analysis method was proved by a Monte-Carlo simulation of the rf recoil spectrometer to be extremely consistent:

The velocity distributions of the evaporation residue nuclei were checked in order to detect the background from reactions of projectiles with target contamination, such as carbon and oxygen. Significant reactions with ^{12}C were found for the reaction ^{40}Ca + ^{16}O. This background reaction is misleading as regards the evaporation of an additional alpha particle. Consequently, the data from this measurement were rejected for analysis.

Table 1. Absolute detection efficiencies of the recoil spectrometer for the reaction ^{40}Ca + ^{19}F in percent

channel	experiment	simulation
2pn	3.0 ± 0.3	4.0 ± 0.4
2p2n	4.5 ± 0.4	4.4 ± 0.5
3pn	4.0 ± 0.4	3.4 ± 0.5
α2p	0.8 ± 0.1	0.7 ± 0.1
2αp	0.8 ± 0.1	0.8 ± 0.1

4 Statistical model calculations

A full computation of the compound nuclei decay according to the principles of the statistical model of nuclear reactions consists of calculating the chances of all concurring decay modes over the range of nuclear excitation for every stage of the de–excitation cascade. This rather complex task requires very substantial computing work. In this paper, the adequacy of different computer codes [see compilation in 10] was examined.

A simple approach is to assume one–step emission and to match barriers and level densities directly with the energy spectra measured. The computer code GANES [11] treats the evaporation cascade in one–step emission by assuming an emitter nucleus with adapted effective excitation energy and effective angular momentum. This code was used by [1,4,5]. The theoretical analysis of compound nuclei with GANES seems to yield extremely low emission barriers for charged particles. We refer here to the controversial interpretations in [2,3] and [4,5].

CASCADE [12], a grid-type code, is well known and widely used. CASCADE calculates inclusive spectra and is not appropriate for channel–specific analysis. We chose CODEX [6], a Monte–Carlo type code. This code permits calculating every experimental observable, e.g. channel–specific energy spectra.

4.1 Implementation

The starting point of the calculation is fusion of the reaction particles. This is calculated according to Bass [13], giving the distribution of the angular momentum of the compound nuclei. The decay cascade is calculated next. The probabilities of the different possible decay modes (emission of nucleon, alpha particle, or gamma) are calculated and determined by chance (fission can be neglected for the reactions handled). The decay calculation is repeated until a ground state is reached.

4.2 Barriers

We calculated transmission coefficients according to the fusion systematics proposed by Vaz and Alexander [14]. These authors systematically investigated fusion cross sections of protons and alpha particles. They used a modified nuclear proximity potential (PP) by introducing a correction parameter δR to the radius R_0 of the tunnelling particles. We took radius correction parameters δR from this approach and estimated their uncertainties. For protons we took $\delta R = -(0.07 \pm 0.03)$ fm, and for alpha particles $\delta R = -(0.04 \pm 0.03)$ fm. The uncertainties concerning the radii lead to uncertainties regarding, the fusion barriers of 130 keV. In addition, we used an optical model potential (OM) [15]. The barriers for protons are 700 keV, and for alpha particles these are 150 keV lower than the values obtained from PP. It becomes clear that a calculation with PP barriers yields "harder" spectra than one with OM barriers.

4.3 Level densities

The level density is a complicated nuclei–specific function of angular momentum and excitation energy. Analytical functions only seem to be practicable for statistical model calculations. In CODEX we used a modified Fermi–gas level density as proposed by Ignatyuk [16] and elaborated further by Schmidt et al. [17]. This formula takes into account shell and pairing energies. These structure–dependent terms are "damped out" with rising excitation energy above the Yrast line. Shell and pairing energies were taken from mass tables compiled by Wapstra and Audi [18].

4.4 Code sensitivity of the analysis

Although the same physics is implemented in the different statistical codes, results differ to some extent. This is due to the differing technical realization. For example, different mesh sizes are used for storing transmission coefficients, level densities and bookkeeping decay nuclei. To check the influence on results, we applied different codes using the same model parameter input as far as possible. Table 3 presents results from CODEX and CASCADE for the reaction ^{40}Ca + ^{19}F. These results give some idea of the practical limits of model calculations.

5 Results

We carried out numerous calculations with CODEX, systematically varying the model parameters in order to reproduce residue distribution and channel–specific energy spectra of protons and alpha particles consistently with one set of parameters.

In agreement with recent publications, we established as a general result that significantly reduced emission barriers relative to the fusion barrier systematics [14] are necessary to reproduce the experimental results obtained from statistical model calculations.

5.1 Angular dependencies

Angular dependencies of the evaporated protons and alpha particles were observed from 110^o to 150^o in the laboratory. Isotropic evaporation was found after transforming the spectra to the center–of–mass system.

5.2 Consistent description of the compound nucleus decay process

The basic idea of this work is to narrow down the selection of model parameters by requiring consistent theoretical reproduction of the experimental data: channel–specific energy spectra of evaporated protons and alpha particles, and evaporation residue distributions.

The model parameters varied were:

- the barriers for proton and alpha particle emission by introducing energy shifts;
- the level density parameter;
- the γ–strength parameter (E1, E2)[see 5.6.1];
- the GDR parameter: resonance energy and width.

We established a set of parameters describing channel-specific energy spectra and evaporation of the reaction ^{40}Ca + ^{19}F simultaneously. This was not possible for ^{40}Ca + ^{12}C. Different emission barriers were necessary for this reaction. No reliable evaporation residue distribution was available (3.2) for the analysis of the reaction ^{40}Ca + ^{16}O.

5.3 Emission barriers

The following table summarizes experimental and theoretical barriers for protons and alpha particles.

Table 2 indicates that OM barriers are closer to the experimental barriers than the PP barriers. The barriers determined for protons and alpha particles are shown in Fig. 5 in a compilation of published data. Two important conclusions can be drawn: The relative reductions of emission barriers are greater for protons than for alpha particles. Channel–specific studies, this paper and [6] show moderate effects in contrast to inclusive studies.

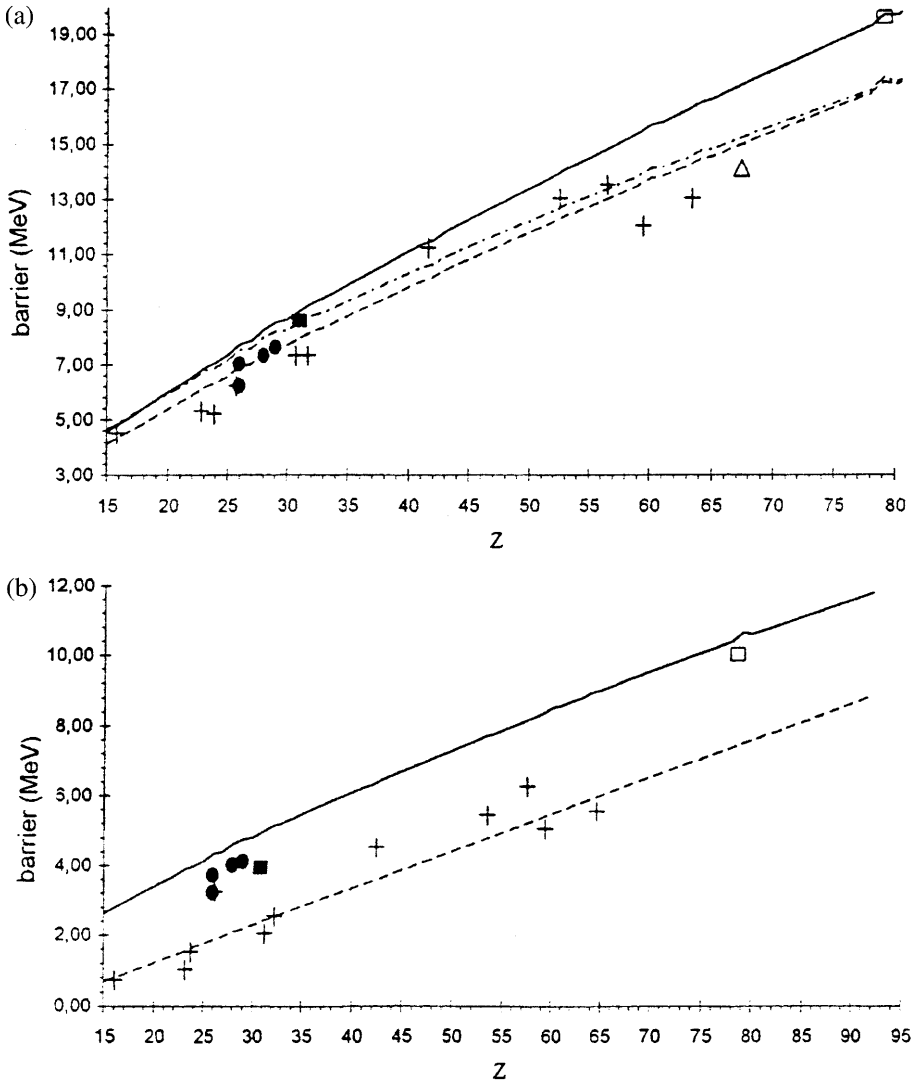

Fig. 5. a Systematics of barriers for alpha particle emission and fusion as a function of the Z of the compound nucleus. The solid line corresponds to the alpha fusion barriers taken from Vaz and Alexander [14]. The dotted line has been obtained by Parker et al. [1]. The authors deduced emission barriers for alpha particles from evaporation energy spectra obtained by inclusive measurements. The dashed–dotted curve was obtained by Alexander et al. [23] from analyzing the mean energies and angular anisotropy for evaporating alpha particles. The barriers calculated refer to stable isotopes yielding e.g. the bump for Z=79. The other symbols correspond to deduced emission barriers for alpha particles from inclusive measurements: crosses data from Parker et al. [1], triangle data from Nebbia et al. [24] solid square data from Majka et al. [25] and channel specific measurements: Open square data from Gollerthan et al. [6] and solid circles data from the present investigation, **b** Systematics of barriers for protons. See Fig. 5a for explanations

Table 2. Barriers in MeV using a modified nuclear proximity potential (PP) and an optical model potential (OM). Experimental barriers were obtained by means of model calculations with CODEX, using optimally adjusted barriers. Maximum errors are estimated to be ± 0.5 MeV. 1) Best suited to reproducing evaporation residue distribution with CODEX. 2) Best suited to reproducing charged-particle energy spectra with CODEX

	PP barriers		OM barriers		Experimental barriers	
compound	p	α	p	α	p	α
^{52}Fe	4.7	7.7	4.0	7.6	$3.2^{1)}$ $3.7^{2)}$	$6.2^{1)}$ $7^{2)}$
^{56}Ni	5	8.3	4.3	8.1	4	7.3
^{59}Cu	5.1	8.4	4.4	8.4	4.1	7.6

5.4 Evaporation residue distributions

Measured evaporation residue distribution and results of model calculations are presented in Tables 3 and 4.

Table 3. Evaporation residue distribution of the reaction ^{40}Ca + ^{19}F. The values are scaled to the sum = 100. 0) indicates CODEX calculations with optimally adjusted barriers. 1) indicates CODEX and 2) CASCADE calculations with the same input parameters and OM (see 4.4). 3) is without GDR (see 5.6.3)

channel	**2pn**	**2p2n**	**3p**	**3pn**
experiment	6.6 ± 0.7	3.8 ± 1	6.8 ± 0.8	29.2 ± 3
0)	8.6	8.4	6.1	29.4
1)	10.4	9.8	7.9	35.4
2)	7.7	5.7	4.2	44.6
3)	4.5	9.6	4.0	39.2
channel	**αpn**	**α2p**	**α2pn**	**αp**
experiment	25.5 ± 5	15.2 ± 1.7	7.9 ± 1.7	5 ± 0.6
0)	18	15.6	4.2	9.8
1)	14.9	14.0	2.6	5.0
2)	14.9	8.1	8.9	5.9
3)	13.5	11.5	9.0	8.7

Table 4. Evaporation residue distribution of the reaction ^{40}Ca + ^{12}C. The values are scaled to the sum = 100. Set 1: Model calculation with the barriers best reproducing the evaporation residue distribution. Set 2: Model calculation with the barriers best reproducing the energy spectra

channel	**pn**	**2p**	**2pn**	**3p**	**αp**	**α2p**
experiment	4.1±0.5	24.6±2.5	14.8±1.5	27.2±3	17.2±3.5	12.3±2.5
set 1	1.9	28.1	14.2	30.2	9.2	16.5
set 2	4.9	44.3	14.3	18.2	11.8	6.4

5.5 Energy spectra of charged particles

The energy spectra of the charged particles in Fig. 6 show generally good reproduction of the experimental distribution in model calculations. One reason for remaining deviations may be due to the model of nuclei–specific level densities implemented in CODEX. Secondly, pre–compound emission may lead to deviations in the higher–energetic region.

5.6 Influence of other physical quantities

5.6.1 Influence of the γ–strength

CODEX does not recognize the parity of γ–transitions and nuclear levels. Effective strengths were therefore used. We carried out model calculations varying effective γ–strength $E_1 = 6.5\ 10^{-4}$ and $E_2 = 5$ Weisskopf units by factors 10^{-2} to 10^2, without revealing any significant influence on the results.

5.6.2 Level density parameter

For the reaction ^{40}Ca + ^{16}O we obtained a = A/9.5 MeV^{-1}, and for ^{40}Ca + ^{16}O a = A/8.4 MeV^{-1}.

For the reaction ^{40}Ca + ^{16}O, we obtained for the best reproduction of the evaporation residue distributions a = A/8.2 MeV^{-1}, and for the best reproduction of energy spectra of light charged particles A/9.3 MeV^{-1}.

These values agree well with Kicinska–Habior et al. [19], suggesting a value of A/9 to A/9.5 MeV^{-1} for nuclei, with A being about 60. A macroscopic calculation according to Töke and Swiatecki [20] yields a level density parameter a = A/6.8 MeV^{-1} for the nuclear mass A = 60. This differs greatly from the experimentally determined values in this paper.

5.6.3 Giant dipole resonance

We found that it is necessary to consider giant dipole resonance (GDR) regarding reproduction of the data. This is shown in Table 3. The γ–emission competes with channels of high nucleon multiplicity, e.g. 3pn in the case of ^{40}Ca + ^{19}F. The GDR reduces the amount of high–energetic evaporated particles. We found a GDR energy of 17 MeV and a resonance width of 10 MeV that match the experimental data. This is in good agreement with a study by Kicinska–Habior and co–workers [19], who investigated γ–emission spectra from the decay of ^{63}Cu at excitation energies from 22.5 to 77.4 MeV.

6 Summary and conclusion

The idea behind this paper is to find out whether the barriers for the emission of light charged particles from a hot nucleus are lower than the barriers for the corresponding fusion reaction of the cold nucleus. An efficient experimental method was developed for detailed channel–specific decay studies for this purpose. This paper shows that the channel-specific data can be reproduced well in model calculations. Slightly lowered emission barriers compared to fusion systematics had to be assumed. But the established reductions of the barriers are not as strong as reported by other authors studying inclusive energy spectra.

We are of the opinion that these inclusive energy spectra investigations may be misleading. The complex multi–step process of compound nuclei decay is observed and analyzed in a rather rough manner. Fusion reactions with target contaminants (^{12}C + ^{16}O) may yield very low-energetic protons and alpha particles, if no selective coincidence is demanded. The very low barriers obtained by Parker et al. [1] may be due to these effects, and they may also be caused by the evaporation code GANES [11] used. This code treats the evaporation cascade as a single emission step by assuming an emitter with an adapted effective energy and angular momentum (c.f. Huizenga et al. [21]). Hence channel–specific studies are necessary, because of their better quality (more details, less background). A crucial point in the theoretical analysis is the choice of the appropriate nuclear potential to obtain the experimental emission barriers. In accordance with the statistical theory of nuclear reactions, transmission coefficients reproducing corresponding fusion experiments (e.g. [14]) have to be used for analysis. But some authors seem to have applied "softer" OM potentials for their calculations. It seems to be more straightforward to apply the systematics proposed by Vaz and Alexander [14]. Another issue is the code dependency found with respect to data analysis. Although we succeed in reproducing the data well with CODEX, we feel that it is important to develop a more advanced code incorporating more nuclear–specific information.

Interestingly enough, the effect of reducing the barriers is stronger for protons (typ.– 20%) than for alpha

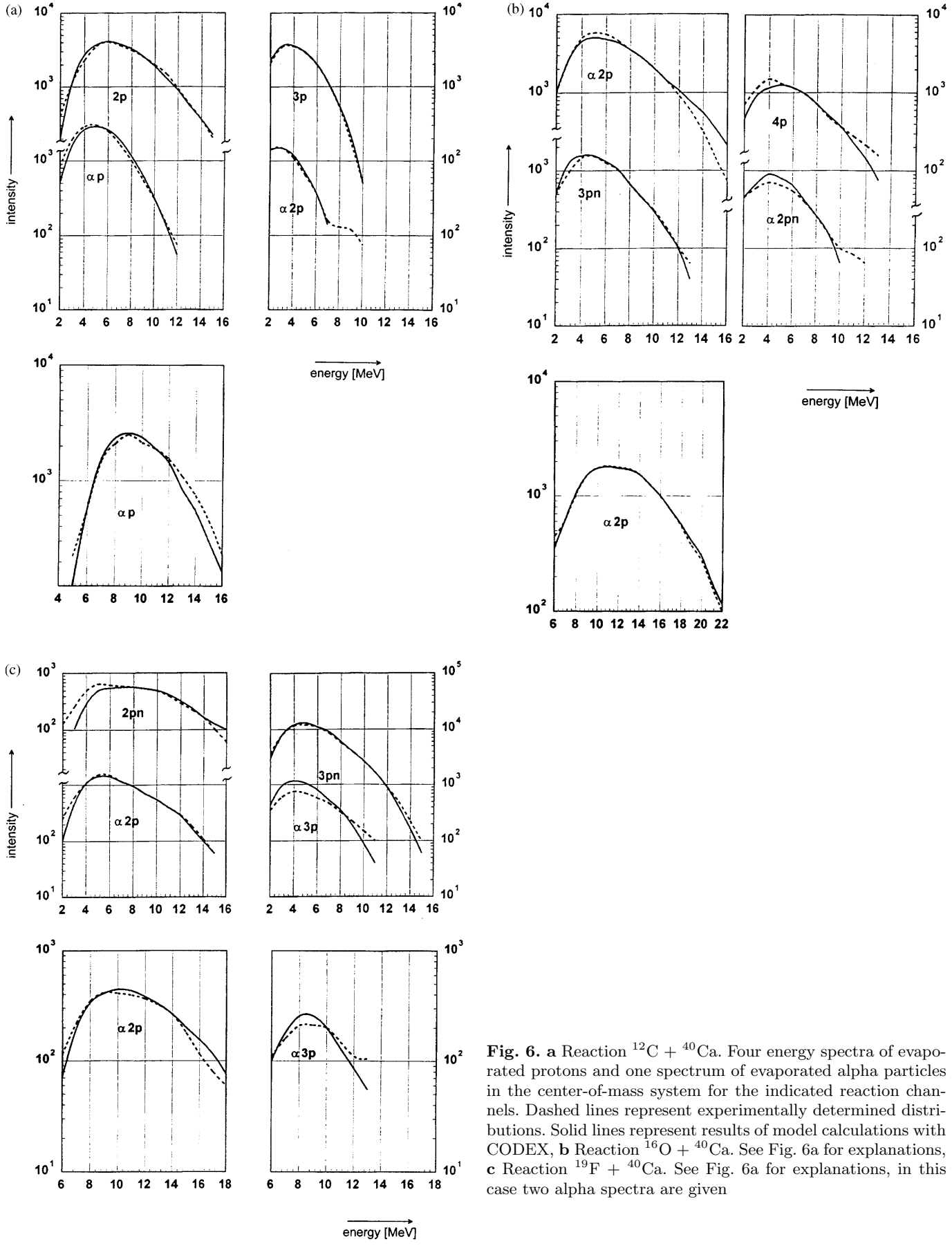

Fig. 6. a Reaction $^{12}C + ^{40}Ca$. Four energy spectra of evaporated protons and one spectrum of evaporated alpha particles in the center-of-mass system for the indicated reaction channels. Dashed lines represent experimentally determined distributions. Solid lines represent results of model calculations with CODEX, **b** Reaction $^{16}O + ^{40}Ca$. See Fig. 6a for explanations, **c** Reaction $^{19}F + ^{40}Ca$. See Fig. 6a for explanations, in this case two alpha spectra are given

particles (typ.– 10%), which indicates that deformation is most likely not the physical origin of the phenomena observed. A possible explanation has been given by Batko et al. [22]. These authors put forward an extended nuclear stratosphere for the excited compound state. According to this model, low–energy protons are favorably emitted from the outer diluted matter distribution, whereas alpha particles are emitted from the inner compact core.

We wish to thank the Tandem staff at the Accelerator Lab in Munich for their professional operation of the accelerator, and Dr. H.J. Maier from the Technological Laboratory of the University of Munich and his staff for having prepared the targets. The authors would also like to thank the staff handling the van–de–Graaff accelerator at the Max Planck Institute for Plasmaphysics at Garching for important energy–calibration measurements. This work has been funded partially by the German Ministry of Research and Technology (BMFT), under Contract Number 06LM171 and the German Research Association (DFG).

References

1. W.E. Parker, M. Kaplan, D. J. Moses, G. La Rana, D. Logan, R. Lacey, J.M. Alexander, D.M. de Castro Rizzo, P. De Young, R.J. Welberry, J.T. Boger, Phys. Rev. C**44**, 774 (1991)
2. I. M. Govil, J.R. Huizenga, W.U. Schröder, J. Töke, Phys. Lett. B**197**, 515 (1987)
3. N.G. Nicolis, D.G. Sarantites, Phys. Rev. C**40**, 2422 (1989)
4. G. La Rana, D.J. Moses, W.E. Parker, K. Kaplan, D. Logan, R. Lacey, J.M. Alexander, R.J. Welberry, Phys. Rev. C**35**, 373 (1987)
5. G. La Rana, R. Moro, A. Bondi, P. Cuzzocrea, A. DOnofrio, E. Perillo, M. Romano, F. Terassi, V. Vardaci, H. Dumont, Phys. Rev. C**37**, 1920 (1988)
6. U. Gollerthan, T. Brohm, H.G. Clerc, M. Horz, W. Morawek, W. Schwab, K.H. Schmidt, F.P. Heßberger, G. Münzenberg, V. Ninov, R.S. Simon, J.P. Dufour, M. Montoya, Z. Phys. A**338**, 51 (1991)
7. K. Rudolph, D. Evers, P.Konrad, K. E.G. Löbner, U. Quade, S.J. Skorka, I. Weidl, Nucl. Instr. and Meth. **204**, 407 (1983)
8. H.H. Anderson and J.F. Ziegler, Stopping Power and Ranges in all Elements, Vol. 3, Vol. 4, Pergamon Press (1977)
9. A. Micholowicz, Kinematics of Nuclear Reactions, lliffe Books, London (1967)
10. G. Stockstad, in Treatise on Heavy–Ion–Physics, Vol.3, edited by D.A. Bromley, Plenum Press New York (1984)
11. N.N. Ajitanand, R. Lacey, G.F. Peaslee, E. Duek, J.M. Alexander, Nucl. Instr. and Meth. A**243**, 111 (1986)
12. F. Pühlhofer, Nucl. Phys. A**280**, 267 (1977)
13. R. Bass, Nuclear Reactions with Heavy Ions, Springer (1980)
14. L.C. Vaz, J.M. Alexander, Z. Phys. A**318**, 231 (1984)
15. C.M. Perey and F.G. Perey, Nucl. Data Tables **10**, 539 (1972)
16. A.V. Ignatyuk, G.N. Smirenkin, A.S. Tishin, Sov.J. Nucl. Phys. **21**, 255 (1975)
17. K.H. Schmidt, H. Delagrange, J.P. Dufour, N. Carjan, A. Fleury, Z. Phys. A**308**, 215 (1982)
18. A.H. Wapstra, G. Audi, Nucl. Phys. A**423**, 1 (1985)
19. M. Kicinska-Habior, K.A. Snover, C.A. Gosett, J.A. Behr, G. Feldmann, H.K. Glatzel, E.F. Garman, Phys. Rev. C**36**, 612 (1987)
20. J. Töke, W.J. Swiatecki, Nucl. Phys. A**372**, 141 (1981)
21. J.R. Huizenga, A.N. Behkami, I.M. Govil, W.U. Schröder, J. Tölze, Phys. Rev. C**40**, 668 (1989)
22. G.Batko, O. Civitarese, Phys. Rev. C**37**, 2647 (1988) 2647i
23. J.M. Alexander, D. Guerreau, L.C. Vaz, Z. Phys. A**305**, 313 (1982)
24. G. Nebbia, K. Hagel, D. Fabris, Z. Majka, J.B. Natowitz, R.P. Schmitt, B. Sterling, G. Mouchaty, G. Berkowitz, K. Strzewski, Phys. Lett. B**176**, 20 (1986)
25. Z. Majka, M.E. Brandan, D. Fabris, K. Hagel, A. Menchaca-Rocha, J.B. Natowitz, G. Nebbia, G. Prete, B. Sterling, G. Viesti, Phys. Rev. C**35**, 2125 (1987)